HHS Public Access

Author manuscript

Cancer Lett. Author manuscript; available in PMC 2021 December 28.

Published in final edited form as:

Cancer Lett. 2020 December 28; 495: 76–88. doi:10.1016/j.canlet.2020.09.004.

Orally available tubulin inhibitor VERU-111 enhances antitumor efficacy in paclitaxel-resistant lung cancer

Foyez Mahmud[a,1], **Shanshan Deng**[a], **Hao Chen**[a], **Duane D. Miller**[a], **Wei Li**[a,*]

[a]Department of Pharmaceutical Sciences, College of Pharmacy, University of Tennessee Health Science Center, Memphis, TN, 38163, USA

Abstract

Lung cancer is the most common cause of cancer associated mortality. Chemotherapeutic agents, such as paclitaxel, are important treatment options but drug resistance often develops upon prolonged use. We report here the preclinical evaluation of a new orally available tubulin inhibitor, VERU-111, which can overcome several ABC-transporter mediated multi-drug resistance associated with taxane treatment. *In vitro*, VERU-111 prevents cell proliferation, invasion, migration and colony formation in both paclitaxel-sensitive and paclitaxel-resistant A549 lung cancer cells. VERU-111 effectively inhibits tubulin polymerization, arrests cells in G2/M phase, and induces cancer cell apoptosis. Further evaluation of various apoptotic proteins revealed that treatment of VERU-111 increases the expression of cleaved-PARP, cleaved-caspase-3 and p-histone H3 proteins. *In vivo*, orally administered VERU-111 in a paclitaxel-sensitive A549 xenograft model strongly inhibits tumor growth in a dose-dependent manner and is equally potent with paclitaxel. When tested in a highly paclitaxel-resistant A549/TxR tumor model, VERU-111 is as effective as the parental A549 model in significantly reducing the tumor volume, whereas paclitaxel is essentially ineffective. Collectively, this study showed that VERU-111 is a promising new generation of anti-tubulin agent for the treatment of taxane-resistant lung cancer.

Keywords

Orally available tubulin inhibitors; Paclitaxel resistance; Colchicine binding site inhibitors; Cell cycle arrest; Lung cancer

*Corresponding Author: Wei Li, University of Tennessee Health Science Center, 881 Madison Avenue, Room 561, Memphis, TN 38163. Phone: 901-448-7532; Fax: 901-448-6828; wli@uthsc.edu.

[1]Present address: Department of Bioengineering, Rice University, 6500 Main Street, Houston, TX 77005, USA.

Author contributions

F.M., D.D.M. and W.L. designed the study. F.M., and S.D. performed experiments. H.C. synthesized and characterized VERU-111. All authors contributed to data analysis and manuscript preparation.

Declaration of competing interest

W.L. is a scientific consultant for Veru, Inc. who licensed VERU-111 for commercial development. W.L. and D.D.M. also report receiving sponsored research agreement grants from Veru, Inc. However, Veru, Inc. did not have any input or influence in the experimental design, data collection, and data analyses in this manuscript. No potential conflicts of interest were disclosed by the other authors.

1. Introduction

Lung cancer related death is expected to remain the highest among all cancer types in the United States in 2020 without sex disparity [1]. Non-small-cell lung cancer (NSCLC) accounts for the major subtype and involves more than 85% of cases among all lung cancer that characterizes distinct pathophysiological features such as adenocarcinoma, squamous and large-cell undifferentiated carcinoma [2]. The standard treatment protocol for lung cancer relies on combination of chemotherapy with radiation therapy and surgical resection. The treatment of lung cancer has been changed dramatically since the discovery of genetic mutations that lead to new targeted therapy or immunotherapy. While these new therapies are revolutionizing lung cancer treatments, currently they only benefit small portions of lung cancer patients who have the desired biomarkers, and chemotherapy still remains a major option for treatments in most lung cancer patients as they can increase the overall survival of stage IIIB-IV NSCLC patients who cannot benefit from targeted or immunotherapies [3]. Combined therapy with different cytotoxic drugs such as cisplatin, pemetrexed, paclitaxel is being frequently used for advanced NSCLC patients [4].

Microtubules are highly dynamic in nature composed with tubulin polymers that acted as key structural components in all eukaryotic cells. They are responsible for various cellular functions including cell migration and mitosis. Thus, targeting microtubules in cancer cells is an important chemotherapeutic treatment strategy that leads to cell cycle arrest in G2/M phase and subsequent cell death [5–7]. Among various microtubule targeting agents (MTAs), paclitaxel is widely used in the treatment of various cancers including lung, breast and ovarian cancers [8–12]. However, the lack of efficacy in its prolonged uses in cancer treatment due to acquired or intrinsic resistance is a widely recognized clinical barrier. Overexpression of certain ATP-binding cassette (ABC) transporters, including the P-glycoprotein (P-gp), multidrug resistance-associated proteins (MRPs), or breast cancer resistance protein (BCRP), can efficiently decrease the intracellular drug accumulation resulting low drug cytotoxicity towards tumor cells [8, 13–16]. Other resistance mechanisms include the altered expression of tubulin isotypes and mutations in the β-tubulin gene. In addition to therapeutic resistance, paclitaxel has dose limiting toxicities such as neurotoxicity, hematologic toxicity or severe hypersensitive reactions, and it also needs to be formulated with a solubilizer (Cremophor EL) due to its low aqueous solubility [17]. Therefore, new generations of tubulin inhibitors are needed to provide more efficacious treatment in patients with NSCLC and other tumor types.

Unlike paclitaxel, tubulin inhibitors that target colchicine binding site in tubulin are more toxic to normal cells but less likely to be at risk for therapeutic resistance. Thus, developing a colchicine binding tubulin inhibitor that will be equally effective with existing chemotherapeutic protocol without significant toxicity and drug resistance would be highly desired. Previously, we have reported that our newly developed VERU-111 (2-aryl-4-benzoyl-imidazole), a relatively safe and potent oral tubulin inhibitor that destabilizes microtubule, was effective in P-gp overexpressing cell lines in both *in vitro* and animal studies (Fig. 1A) [18]. Distinct from paclitaxel and vinorelbine, VERU-111 binds to the colchicine site in tubulin. Extensive studies have shown that VERU-111 effectively suppresses tumor growth and metastasis in human melanoma (A375), prostate cancer (PC-3

and DU-145), pancreatic cancer (AsPC-1), and breast cancer (HCI-10 and MDA-MB-231) xenograft models [18–21]. Currently, VERU-111 is under Phase 1B/2 clinical trials for patients with castration-resistant prostate cancer [NCT 03752099]. To evaluate if VERU-111 as an oral tubulin inhibitor is effective in lung cancer models, we have carried out *in vitro* and *in vivo* experiments using both paclitaxel-sensitive (A549) and paclitaxel-resistant lung cancer cell lines (A549/TxR). Xenograft studies revealed that orally active VERU-111 showed lower side effects and superior therapeutic benefits over paclitaxel therapy in resistant lung cancer model. Our reported results here clearly demonstrate that VERU-111 is a promising new generation anti-tubulin agent for the treatment of paclitaxel-resistant lung cancer.

2. Materials and methods

2.1. Cell culture and reagents

Human lung cancer cell lines A549 (NSCLC), HCC827, H460, and H1299 were obtained from American Type Culture Collection (ATCC, Manassas, VA) and cultured in RPMI 1640 medium (Gibco, Carlsbad, CA) containing mixture of 10% fetal bovine serum (FBS, Atlanta Biologicals, Lawrenceville, GA) and 1% antibiotic/antimycotic solution (Sigma-Aldrich, St. Louis, MO). The cells were maintained to 80–90% confluency at 37 °C temperature with 5% CO_2 in a humidified atmosphere. Paclitaxel-resistant variant of NSCLC A549/TxR cell was derived by the continuous treatment with paclitaxel in nanomolar range (2–150 nM). Paclitaxel treatment was gradually increased from very low concentration and continued for 3–5 days in A549 parenteral cell lines. Meanwhile, the cells were allowed to recover by replacing with drug free culture medium. A549/TxR subline was maintained with the same culture medium containing paclitaxel and shifted with drug-free media a week before actual experiment. Stable A549/TxR cells (IC_{50} = 5411.0 nM) were generated in 2.5–3 months.

VERU-111 was synthesized and characterized according to the previous published protocol [18]. For *in vitro* studies, VERU-111, paclitaxel or colchicine were prepared in DMSO (ATCC) at a stock concentration of 20 mM and stored in −20 °C in a freezer. Prior to experiments, stock was diluted with the proper culture medium and the final concentration DMSO in drug solution was maintained below 1%.

2.2. Cytotoxicity assay

Depending on their growth rate, cancer cells were seeded at a concentration of 2.5–5 × 10^3 cells per well in 96-well plate. On next day, the culture medium was replaced with the fresh medium containing the test compounds at different concentrations in six to eight replicates. After 72 h of incubation, 20 μL of MTS [3-(4,5-dimethylthiazol-2-yl)-5-(3-carboxymethoxyphenyl)-2-(4-sulfophenyl)-2H-tetrazolium, inner salt] reagent (Promega, Madison, WI) was added to the each well in dark and incubated at 37 °C for 1–3 h depending on the cell types. Absorbance was recorded at 490 nm using a microplate reader (BioTek Instruments Inc., Winooski, VT). The half maximal inhibitory concentration (IC_{50}) values were calculated by GraphPad Prism software (San Diego, CA).

2.3. Clonogenic survival assay

Paclitaxel-sensitive A549 and paclitaxel-resistant A549/TxR cells were seeded in 6-well plates at a low concentration (500 cells/well). Cells were allowed for attachment overnight at 37 °C, treated with a compound (paclitaxel, colchicine or VERU-111) at different concentrations (0 nM, 4 nM and 16 nM), and incubated for additional 10 days. Colonies were then fixed with 10% formalin solution for 10–20 min and stained with 0.1% (w/v) crystal violet for 30 min. The excess dye was removed and washed with tap water. The plates were air-dried, and the images were taken with Evos Fl imaging system (Life Technologies, Carlsbad, CA).

2.4. Wound healing and invasion assay

Paclitaxel-sensitive A549 and paclitaxel-resistant A549/TxR cells were seeded into the 12-well plates at a cell density of 1×10^5/well and incubated overnight. To create uniform identical scratches, a 200 μL pipet tip was used to make a straight line through the attached cells. Cellular debris was removed, and the wells were replaced with drug-free medium or fresh medium containing 25 nM single concentrations of VERU-111, paclitaxel, or colchicine. The photographs were taken at 36 h after drug incubation. Cell invasion assay was done in 24-well Matrigel Invasion Chambers (Corning, Biocoat) according to the manufacturer's protocol. Serum free medium containing 1×10^5 A549 or A549/TxR cells were added into top chamber and treated with 25 nM of different test compounds for 48 h. Medium containing 10% FBS was used as chemoattractant and the invaded cells in lower chamber were fixed with ice-cold methanol, stained with 0.5% crystal violet solution and captured by a microscope.

2.5. Analysis of efflux transporter overexpression

2.5.1. Cellular expression of P-gp protein by western blotting—Cell lysates of A549 or A549/TxR cells were prepared with ice-cold RIPA buffer containing protease inhibitor cocktails in standard procedure. The total protein from the whole cell lysates was determined by BCA methods as per manufacturer instructions. Equal amount of protein was resolved on 10% SDS-PAGE gel electrophoresis and transferred onto PVDF membrane. Following protein transfer, the membrane was blocked with 5% skim milk in TBST and probed with primary antibody mouse anti-P-gp (Invitrogen, catalog #MA1–26528) overnight followed by the secondary antibody conjugated with horseradish peroxide (Cell signaling, catalog #7076). Images were developed by chemiluminescence method using ChemiDoc-It2 Imaging System (Bio-Rad, Hercules, CA).

2.5.2. Intracellular Rh-123 uptake—Rhodamine-123 accumulation (Rh-123) in A549 or A549/TxR cells was measured by flow cytometric analysis (FACS) according to the previously published report [22]. Cells were seeded in 6-well plates, treated with 10 μM Rh-123, and co-incubated with verapamil as a positive control or VERU-111 for 24 h. After washing off unbound dye, cells were re-suspended and kept in the dark until FACS. Rh-123 uptake in the lung cancer cells that cultured in glass coverslip was further confirmed by cellular staining using a fluorescence microscope.

2.6. Immunofluorescence staining

Sub-confluent A549 cells growing for overnight on glass coverslips in 6-well plates were treated with paclitaxel, colchicine or VERU-111 at a concentration of 100 nM for 24 h. After washing with PBS, cells were fixed with 4% paraformaldehyde (PFA) and permeabilized with 0.1% triton X-100 in PBS solution. Microtubules were stained with an anti α-tubulin antibody (Thermo Scientific, Rockford, IL) for overnight at 4 °C, followed by incubation with Alexa Fluor 647 goat anti-mouse IgG (catalog #A32787, Molecular Probes, Eugene, OR) at room temperature for 1h. The coverslips were washed three times with PBS and mounted in a glass slide with DAPI containing Vectashield antifade mounting media (catalog #H-2000, Vector Lab., Burlingame, CA). The photographs were acquired with a Keyence BZ-X700 fluorescence microscope (Osaka, Japan).

2.7. Cell cycle and apoptosis analysis

In order to determine the effects of VERU-111 on cell cycle distributions, A549 lung cancer cells were seeded in 6-well plates and incubated with 100 nM of drug solutions for 24 hours. Cells were then harvested with trypsin and fixed in ice-cold ethanol (70%) overnight. Subsequently, cells were resuspended with 100 μg/mL RNase A (Sigma-Aldrich, St. Louis MO) and the DNA was stained with 50 μg/mL propidium iodide (PI) in PBS solution under dark condition. For apoptosis assays, the live cells were treated with annexin V-FITC solution according to the manufacturer instructions (Apoptosis detection kit, BD Biosciences, San Jose, CA). The data acquisition was done by Bio-Rad ZE5 flow cytometer (Bio-Rad, Hercules, CA) and data analysis was performed by ModFit LT or FlowJo v10.3 software.

2.8. Western blot analysis

A549 or A549/TxR cells were seeded on tissue culture dishes for overnight followed by 100 nM paclitaxel or 100 nM VERU-111 treatment for 24 h. For time-dependent studies, cells were exposed with 100 nM VERU-111 for 24, 36 and 48 h. After treatment, cells were harvested, lysed in RIPA buffer with Halt™ protease and phosphatase inhibitor (Thermo) and centrifuged at 13,000 rpm for 10 min. Supernatant was collected, and Bradford method was used for protein quantification (Bio-Rad, Hercules, CA). 50 μg of denatured protein samples were electrophoretically separated by 10% SDS-PAGE polyacrylamide resolving gels and transferred to a PVDF membrane. The membranes were blocked for 1 h in 5% non-fat milk in TBST solution, followed by the overnight incubation with primary antibodies at 4 °C; rabbit anti-cleaved-PARP (1:1000), anti-cleaved-caspase-3 (1:1000), anti-p-AKT (1:1000), anti-p-histone H3 (1:1000) and anti-GAPDH HRP conjugate (1:2000) (catalog #5625; #9661; #4060; #9701; #3683, respectively, Cell Signaling Technology, Danvers, MA). After washing three times with TBST solution, the membranes were incubated with peroxidase-conjugated anti-rabbit IgG secondary antibody (1:2000, #7074, Cell Signaling Technology). The membranes were washed with TBST for three times, visualized with Clarity™ Western ECL Substrate (Bio-Rad, #1705060) and exposed to X-ray films for visualization of the protein bands. The positive bands were analyzed with Image Studio Lite software.

2.9. In vivo xenograft model

All animal experiments followed the guidelines from the National Institute of Health and the protocol was approved by the Institutional Animal Care and Use Committee (IACUC) at the University of Tennessee Health Science Center (UTHSC, Memphis, TN). Female athymic nude mice (6–8 weeks old) were purchased from Envigo and maintained under controlled environmental conditions in the animal facility. A549 human lung cancer cells were suspended in medium and diluted with Matrigel immediately before the injection. Then, 8×10^6 A549 cells in 100 μL were inoculated in the right flank of each mouse. The drug treatments were initiated when the tumor reached around 100 mm^3. Tumor volume was measured using a caliper and calculated as $a \times b^2 \times 0.5$, where a and b represented the larger and smaller dimensions of the tumors, respectively. Paclitaxel was dissolved in ethanol and diluted in a 1:1:18 ratio of ethanol:Cremophor EL:PBS solution. VERU-111 was first dissolved in PEG300 and further diluted in distilled water in a ratio of 3:7. All drug solutions were diluted prior to administration of mice from the stock solution. There were total four groups were used in this animal study, (a) vehicle treatment, (b) paclitaxel intraperitoneal (ip) injection of 12.5 mg/kg three times per week (3x/wk, every other day), (c) VERU-111 orally (po) administered 7.5 mg/kg 5 days in a week, and (d) VERU-111 (po) 12.5 mg/kg 5 days in a week.

For the paclitaxel-resistant A549/TxR model, the tumor inoculation and study procedure remained the same as above. However, there were two additional groups that included in this experiment; cisplatin 5 mg/kg ip once weekly and the combination of cisplatin and VERU-111 at a dose of 12.5 mg/kg. Cisplatin solution was prepared into warm normal saline solution under sterile condition.

2.10. Immunohistochemistry

The excised tumor tissues and other major organs were collected in 10% formalin solution and embedded in paraffin. Serial sections were obtained, de-paraffinized, and stained with hematoxylin and eosin (H&E). The immunohistochemistry (IHC) staining was performed with rabbit anti-cleaved-caspase-3 antibody (Cell Signaling Technology Inc.), rabbit anti-Ki-67 and rabbit anti-CD31 (Cell Signaling Technology) following ABC-DAB methods. Antigen retrieval was performed with H-3300 antigen unmasking solution (Vector Laboratories, Burlingame, CA). Slides were imaged and analyzed with a Keyence BZ-X700 microscope and BZ-X analyzer software (Osaka, Japan).

2.11. Statistical Analysis

All data were analyzed using GraphPad Prism 7.0. Data were provided as the mean ± SEM unless otherwise indicated. The statistical significance ($p < 0.05$) was calculated by one-way ANOVA and Student's t-test.

3. Results

3.1. VERU-111 demonstrates potent cytotoxicity in lung cancer cells including paclitaxel-resistant subline

The cell viability assay was performed to assess the efficacy of VERU-111 on different lung cancer cell lines. VERU-111 showed similar potency in comparison with that of colchicine (Supp. Fig. S1A–E). Moreover, VERU-111 had excellent inhibitory activity in nanomolar range against different phenotypes of lung cancer cell lines, such as, HCC827 (EGFR mutated epithelial adenocarcinoma), H1299 (P53 negative NSCLC), A549 (NSCLC), and H460 (P53 positive epithelial large cell carcinoma). Among these paclitaxel-sensitive cell lines, paclitaxel exhibited the highest potency (0.37– 73.55 nM) among these three tubulin inhibitors. However, both paclitaxel and colchicine were ineffective in paclitaxel-resistant cell line (A549/TxR) and the resistance index (RI) was 287.8 and 6.7, respectively (Table 1). In contrast, VERU-111 showed similar potency to induce cell death on parenteral A549 and resistant A549/TxR cell lines with IC_{50} values of 55.6 nM and 102.9 nM, respectively, and the RI was only 1.9. Since P-gp has been showed overexpressed in many paclitaxel-resistant tumors, the results indicated that VERU-111 could overcome clinically relevant paclitaxel resistance in lung cancer.

3.2. VERU-111 inhibits the colony formation in lung cancer cells

When a small number of cells were added to the culture plate, they started to proliferate and become a colony that enables to evaluate the potential anti-proliferative effects from drug candidate. The results revealed that VERU-111 showed the reduction of new colony formation and suppressed the cancer cell growth for a longer period (10 days) in 16 nM drug concentration (Fig. 1B). In A549 cells, treatment with 4 nM and 16 nM of VERU-111 resulted in 9.1% and 0.98% of colony covered area, whereas, the colonies from the control group occupied 15.9% of the total surface area (Fig. 1C–D). As expected, paclitaxel-treated cell was most effective and demonstrated the partial growth inhibition at 4 nM and the complete growth inhibition at 16 nM concentrations. Both VERU-111 and paclitaxel treatment groups in higher drug concentration demonstrated comparable inhibitory effects of colony formation and the results were significant ($p = 0.028$ for VERU-111 and $p = 0.0029$ for paclitaxel). In case of A549/TxR cells, both paclitaxel and colchicine failed to control colony formation, whereas, VERU-111 retained its ability to inhibit colony formation (1.9%, $p = 0.0023$) in this highly paclitaxel resistant phenotype.

3.3. VERU-111 suppresses invasion and migration of the lung cancer cells

Similarly, wound healing assays revealed that VERU-111 had comparable efficacy to inhibit the cell migration with paclitaxel, and significantly higher efficacy than colchicine-treated group in sensitive A549 cells ($p = 0.0286$). After 36 hours, the control cell completely covered the scratch area, and the treatment with paclitaxel, colchicine, and VERU-111 groups were demonstrated 47.8%, 64.6%, and 50.3% of the wound closure from the initial scratch area, respectively (Fig. 1E). In contrast, the positive control groups were unable to stop the migration process in A549/TxR cells. But, VERU-111 demonstrated significantly higher inhibition of wound closure (50.89%, $p = 0.002$ vs. colchicine, and $p = 0.024$ vs. paclitaxel) compared with the positive controlled-treated groups (Fig. 1F–G). In addition,

the cell invasive capability of VERU-111 was also determined by using matrigel coated transwell membrane. After 48 hours of drug treatment, the invading cells from the lower chamber were stained and the images were quantified by ImageJ software. The results indicated that all three treatment groups showed marked inhibition of A549 cell invasion compared with the vehicle control (Fig. 2A). The results from the VERU-111 and paclitaxel agreed with the migration study and found statistically significance ($p = 0.028$ to VERU-111 and $p = 0.0025$ to paclitaxel). In case of resistant cell line, treatment with VERU-111 exhibited 33.06% of invaded cells compared with control group while the capacity of paclitaxel and colchicine to suppress the cell invasion was negligible (Fig. 2B–C).

3.4. VERU-111 is not a substrate for P-gp efflux protein

It is well-known that one of the mechanisms of drug resistance associated with MTAs is the overexpression of membrane-bound efflux proteins such as P-gp protein. To confirm that our developed A549/TxR daughter line has this clinically relevant drug resistance, we investigated P-gp expression in this paclitaxel-resistant cell line. Western blot analysis revealed that P-gp was indeed highly expressed in A549/TxR cell line compared with its parental A549 cell line (Fig. 3A). Result from flow cytometry also confirmed this observation and found much lower accumulation of Rh-123 into A549/TxR cells because of Rh-123 acts as a P-gp substrate and thereby was pumped out from the cells (Fig. 3B). When co-incubated with verapamil which is a known P-gp inhibitor, the concentration of Rh-123 become significantly higher in A549/TxR cells. Figure 3C showed 76.7% of Rh-123 positive cells in compare with 3.18% cells of that in control. Co-incubation with verapamil and Rh-123 showed slight increment of Rh-123 uptake in sensitive cells but significantly higher in resistant cells ($p = 0.0165$ vs. control) suggesting low presence of P-gp in parenteral cell lines. As shown in figures 3D and 3E, VERU-111 had no influence on the Rh-123 uptake and thus it was not considered as P-gp substrate.

3.5. VERU-111 interferes with microtubule polymerization

To evaluate effects of VERU-111 on microtubule polymerization in A549 cells, we employed two known positive controls: paclitaxel (stabilizing microtubules) and colchicine (destabilizing microtubules). Immunofluorescence study revealed that the control cells showed the regular morphology with the typical microtubule network that distributed evenly throughout the cell cytoplasm in an organized manner. In contrast, cells treated with either VERU-111 or colchicine enhanced the soluble tubulin protein accompanied with depolymerized and fragmented microtubules (Fig. 4), while cells treated with paclitaxel caused ring-like concentrated microtubule bundling around the cell nuclei resulted from its ability to induce stabilization of polymerized microtubules.

In A549/TxR cells, both paclitaxel and colchicine-treated groups displayed similar microtubules networks that are comparable with the vehicle controlled group, indicating their loss of effectiveness in disruption of microtubule dynamics in these paclitaxel-resistant cells. In contrast, VERU-111 maintained its ability to cause the disruption of microtubule networks and increased microtubule fragmentation. Taken together, VERU-111-treated group showed similar potency to disrupt microtubule dynamics in both sensitive and

resistant subtypes that led to its potential therapeutic application for paclitaxel-resistant lung tumors.

3.6. VERU-111 produces cell cycle arrest at the G2/M phase in A549 and A549/TxR cells

To test whether VERU-111 directly involves with the cell cycle arrest in lung cancer, we performed flow cytometry experiment using PI staining. It is well documented that paclitaxel therapy blocks the G2/M phase in cell cycle leading to significant apoptosis as indicated by the subG1 fraction [11]. We observed comparable G2/M cell cycle arrests when A549 cells were incubated with 100 nM of paclitaxel (35.4 ± 6.1%), colchicine (37.8 ± 6.4%), or VERU-111 (47.4 ± 9.5%) for 24 hour, but significantly higher effects compared with untreated cells (7.7 ± 3.9%) (Fig. 5A, 5C). Similar effects of VERU-111 were also observed in A549/TxR cell lines ($p = 0.0043$), whereas treatment with either paclitaxel or colchicine failed to produce significant G2/M phase arrest (Fig. 5B, 5D). We next examined the abilities of these compounds to induce apoptosis. While cells treated with the vehicle control in parental A549 exhibited only 4.4% of late stage apoptotic population (both annexin V and PI positive cells), treatment with paclitaxel, colchicine, or VERU-111 showed, 7.8%, 10.9%, and 12.1% apoptotic events, respectively (Fig. 5E).

3.7. Western blot analysis

In order to identify the intrinsic apoptotic pathway of VERU-111, we analyzed different apoptotic proteins in the cellular level. The results indicated that VERU-111 significantly increased the expression of cleaved-caspase-3 in both sensitive and resistant cell lines. In addition, VERU-111 also up-regulated both cleaved-PARP and p-histone H3, whereas it reduced the expression of p-AKT proteins (Fig. 5F). It is important to note that both caspases and PARP are the significant mediators for the induction of cellular apoptosis. In addition, VERU-111 showed time-dependent enhancement of cleaved-PARP protein in both lung cancer cell lines (Fig. 5G). From the western blot data, the phosphorylation level histone H3 also increased in both A549 and A549/TxR cells, indicating the cell cycle arrest occurred in mitosis phase. Interestingly, VERU-111 greatly decreased the phosphorylation of AKT which negates the recovery the tumor cells from the apoptosis. Paclitaxel showed the similar mechanism only in A549 cells, but it failed to modulate p-AKT in A549/TxR cells.

3.8. Antitumor efficacy study

In the A549 tumor xenograft model, both 7.5 mg/kg and 12.5 mg/kg doses of VERU-111 significantly demonstrated dose-dependent antitumor efficacy compared with the vehicle (Fig. 6A–D). Among them, 12.5 mg/kg oral dose of VERU-111-treated group had comparable efficacy with paclitaxel-treated group in terms of tumor volume and the final tumor weight. Body weight of mice from different treatment groups revealed that none of these drugs with this dose range and frequency were toxic. Likewise, VERU-111 exhibited strong tumor suppression in the resistant A549/TxR xenograft model (Fig. 6E–H). Treatment with an oral dose of 7.5 mg/kg and 12.5 mg/kg of VERU-111 showed 69.0% and 77.7% of tumor inhibition ($p = 0.0008$ for 7.5 mg/kg, and $p = 0.0001$ for 12.5 mg/kg). In this experiment, cisplatin treatment was also included as positive control group, and it demonstrated 70.1% tumor inhibition in lung cancer. The greatest tumor reduction was

observed in combination of 12.5 mg/kg of oral VERU-111 and 5 mg/kg of ip cisplatin-treated group. However, the combination group was also demonstrated slight reduction of mice body weight indicating cisplatin induced toxicity to mice and similar loss of body was also observed in cisplatin therapy group alone. However, there was no animal mortality observed during the study period. In this xenograft model, paclitaxel group displayed negligible tumor inhibition effect compared to vehicle group suggesting paclitaxel therapy was essentially ineffective in paclitaxel-resistant tumor model.

3.9. Immunohistochemistry in tumor tissues of A549/TxR xenograft model

H&E stained slides from the vehicle group demonstrated that very dense tumor cells comprising proliferating mitotic cells were observed by intense hematoxylin staining. A similar result was also found in paclitaxel-treated group that indicated the taxane therapy was ineffective. However, treatment with VERU-111, cisplatin, or their combination exhibited higher necrosis area in the A549/TxR tumors, and less cell proliferation and this effect was further confirmed by the Ki-67 antibody staining (Fig. 7). Immunohistochemistry in the tumor tissue was also conducted to evaluate the tumor cell apoptosis and the proliferation of the tumor endothelial cells. Cleaved-caspase-3 staining demonstrated that the vehicle tumor had fewer apoptotic cells compared with the treatment with VERU-111 or cisplatin. This result was also in agreement with our previous findings where VERU-111-treated groups showed enhanced G2/M phase arrest cells during the cell cycle analysis resulting increased apoptotic cells in the tumor. To survive and maintain the nutritional demand, tumor cells must recruit the endothelial cells to remodel the networks of blood vessel. Thus, we also evaluated the status of blood vessel inside the tumor using CD-31 antibody staining. The result indicated that the vehicle or paclitaxel-treated group showed uniform network of blood vessel in tumor, while treatment with VERU-111 or in combination with cisplatin demonstrated very few positive areas of blood vessel confirming the anti-angiogenic effects of VERU-111.

4. Discussion

Microtubules are one of the most essential cellular components and fundamentally responsible for structural scaffolds, mitosis, cellular transport and intracellular signaling. Microtubules possess highly dynamic instability and vary during cell division, and this makes them an attractive target for the treatment of various cancers [23]. Although taxanes (such as paclitaxel and docetaxel) serve as an important treatment strategy for decades in lung, breast, ovarian cancer including other human malignancies, paclitaxel therapy often becomes ineffective by the increased frequency of the drug resistance and mutation in drug targets [24, 25]. Therefore, new generations of tubulin inhibitors that can overcome paclitaxel resistance could have high impact in taxane-resistant lung cancer. Previously, we have reported that VERU-111 as an orally bioavailable tubulin inhibitor could effectively bypass the P-gp mediated efflux transporter in prostate cancer and breast cancer models [21, 26, 27]. Unlike paclitaxel, VERU-111 binds with the colchicine binding site and thereby promotes depolymerization of microtubules [18]. Mounting evidence suggests that colchicine binding agents showed several advantages over the other tubulin inhibitors, such as less prone to ABC efflux transporters, higher water solubility and lower molecular weight

that all contributes to enhanced oral bioavailability [28]. Consistent with this, VERU-111 has been reported to have satisfactory oral bioavailability (21 ~ 50 %) in both small and large animal models and acceptable aqueous solubility [29].

Herein, we investigated the effects of VERU-111 in paclitaxel-sensitive and paclitaxel-resistant lung cancer cell lines. The cell viability assay demonstrated the comparable efficacy of VERU-111 with paclitaxel and colchicine, and the IC_{50} value showed 29.0 nM to 178.0 nM ranges in four paclitaxel-sensitive lung cancer lines. To test VERU-111 against drug resistance model, stable paclitaxel-resistant A549/TxR cells were developed by repeated exposure of low concentration of paclitaxel in culture media for 2.5–3 months period. MTS assay revealed that the normal susceptibility towards paclitaxel treatment was completely lost and this was also partially true for colchicine. However, VERU-111 showed similar cell viabilities in both sensitive A549 and resistant A549/TxR cells. Next, we wanted to test the ability of VERU-111 on cancer cell colony formation using the same lung cancer cell lines. VERU-111 demonstrated dose-dependent inhibition of cell colony formation in both sensitive and resistant cell lines. In contrast, paclitaxel or colchicine treatments were not effective in A549/TxR cell lines. Similar findings were also observed in wound healing assay where all three drug treatments delayed the A549 lung tumor cell migration but failed in resistant A549/TxR cells except VERU-111. Further *in vitro* experiments for studying the angiogenesis and metastasis of cancer cells have been carried out. We used matrigel-coated transwell chamber that contains various extracellular matrix (ECM) and growth factors to study the nature of invasiveness of the lung cancer cell lines. Our *in vitro* data from invasion assay showed that VERU-111 reduced the recruitment of cells across the porous membrane in presence of chemoattractant, indicating tumor metastasis might be inhibited with VERU-111. Indeed, VERU-111 also effectively controlled cell invasion in resistant cells while no significant changes were observed in the paclitaxel or colchicine treated groups.

Martello et al. reported that A549 paclitaxel-resistant cell lines required low concentration of paclitaxel to restore their normal cellular function along with microtubule dynamicity and this effect might be related with the overexpression of specific βIII-tubulin isotype [30]. In general, paclitaxel-resistant cells also demonstrated the abundance expression of βIII-tubulin compared with its sensitive counterpart [31]. In the case of our developed A549/TxR cells, their normal cellular growth did not depend on continuous presence of paclitaxel in culture media. Thus, higher expression of an efflux transporter such as P-gp is most likely to be involved in drug resistance in A549/TxR cell line. Other researchers have also confirmed that a plausible resistance mechanism is the overexpression of various ABC transporters that led to efflux of taxanes out of the cancer cells. Among them, P-gp mediated drug resistant is the one key contributing factor for paclitaxel inactivity in cancer treatment [22, 32, 33]. Therefore, we used western blot method to analyze the status of P-gp protein expression in A549 cells. The result indicated that resistant cells had significantly higher expression of P-gp compared with sensitive cells which could be the main driving force for paclitaxel resistance. To further confirm this, we used Rh-123, a well-known tracer dye for P-gp, alone or in combination with a test drug into the cells. Accumulation of Rh-123 in parental A549 cells was much higher compared with resistant cells indicating the presence of P-gp in A549/TxR cells (Supp. Fig. S2). Incubation with VERU-111 did not affect the uptake of Rh-123 into either A549 or A549/TxR cells, suggesting its ability to circumvent P-gp

mediated drug resistance. Further flow cytometry studies revealed that VERU-111 was not a substrate for P-gp. This finding correlates with our previous reports for VERU-111 [21].

Immunofluorescence study of the microtubule showed the abnormal microtubule morphology in drug-treated groups. Specifically, paclitaxel-treated A549 cells displayed microtubule bundling phenotypes which is a typical signature of microtubule stabilizing agents [34]. In contrast, both VERU-111 and colchicine showed abnormal microtubule organization or depolymerization. In A549/TxR resistant cell lines, microtubules from control, paclitaxel and colchicine-treated cells exhibited normal morphologies with normally distributed microtubule filaments around the cytoplasm, while VERU-111 treated cell maintains its ability to disrupt microtubule dynamics. MTAs have been extensively reported to induce their anticancer effects by strongly arrest cells in G2/M phase. During cell cycle analysis in parental A549 cells, all the treatment groups induced G2/M cell cycle arrest; however, only VERU-111 showed the G2/M phase arrest in resistant cell lines. Similarly, apoptosis was significantly increased in A549 cells treated with all three tubulin inhibitors. However, VERU-111 was the only tubulin inhibitor that was able to induce growth arrest in A549/TxR cells. We further investigated the apoptosis pathway caused by the VERU-111 treatment. Western blot analysis revealed that enhanced apoptosis was related with the upregulation of cleaved-caspase-3 which was accompanied by cleaved-PARP. Up-regulation of p-histone H3 also indicated the apoptosis occurred primarily in the mitosis phase of the cell cycle. The phosphorylation of AKT protein was dramatically decreased by VERU-111 treatment, demonstrating it interference with the cellular signaling pathway.

Unlike taxane, VERU-111 is an orally available agent that has several advantages over conventional maximum tolerated dose (MTD) based intravenous drugs, such as, prolonged plasma drug concentration, reduced toxicity and convenient frequent dosing making it more patient friendly and inexpensive [35, 36]. In xenograft studies, oral administration of VERU-111 showed significant growth inhibition in both A549 and A549/TxR tumors. The body weight from VERU-111-treated mice exhibited normal limit indicating that the therapy with VERU-111 was safe. It is important to note that paclitaxel therapy is often associated with dose limiting toxicity such as neurotoxicity, myelosuppression and other adverse effects [37]. In resistant A549/TxR tumors, paclitaxel could not suppress the tumor growth and the result is consistent with the *in vitro* findings. In most cases, treatment of lung cancer relies on the use combination chemotherapeutics which include platinum-based therapy [3, 38]. Thus, we also tested cisplatin therapy in combination with VERU-111 in a xenograft study. The result indicated that the combination therapy was the most effective treatment in controlling the tumor growth among all of the treatment groups. Further, immunostaining in tumor sections confirmed that the treatment with VERU-111 or in combination with cisplatin increased the apoptosis and necrosis in lung tumors, reduced tumor cell proliferation, and disrupted new blood vessel formation in tumors compared with vehicle-treated group. Thus, VERU-111 showed superior anticancer activity as single agent or in-combination with cisplatin in both sensitive A549 and paclitaxel-resistant A549/TxR lung cancer models.

In conclusion, we have evaluated an orally available tubulin inhibitor with superior therapeutic benefits over existing paclitaxel therapy. VERU-111 interacted with the

colchicine binding site, and it had much less susceptibility for P-gp mediated drug resistance. *In vitro* studies demonstrated that VERU-111 induced cell apoptosis through G2/M phase cell cycle arrest and cancer cell apoptosis. VERU-111 showed similar antitumor efficacy in both paclitaxel-sensitive and paclitaxel-resistant lung tumors. Collectively, results presented in this study demonstrated that VERU-111 is a strong drug candidate for improved treatment in lung cancer.

Supplementary Material

Refer to Web version on PubMed Central for supplementary material.

Acknowledgments

This work was supported by the NIH grant R01CA148706 (to W. Li and D. D. Miller). The contents of the article are solely the responsibility of the authors and do not necessarily represent the official views of the NIH.

References

[1]. Siegel RL, Miller KD, Jemal A, Cancer statistics, 2020, CA: Cancer J. Clin 70 (1) (2020) 7–30. [PubMed: 31912902]

[2]. Meza R, Meernik C, Jeon J, Cote ML, Lung cancer incidence trends by gender, race and histology in the United States, 1973–2010, PloS one 10 (3) (2015) e0121323. [PubMed: 25822850]

[3]. Schiller JH, Harrington D, Belani CP, Langer C, Sandler A, Krook J, et al., Eastern Cooperative Oncology, Comparison of four chemotherapy regimens for advanced non-small-cell lung cancer, N. Engl. J. Med 346 (2) (2002) 92–98. [PubMed: 11784875]

[4]. Nawaz K, Webster RM, The non-small-cell lung cancer drug market, Nat. Rev. Drug Discov 15 (4) (2016) 229–230. [PubMed: 27032828]

[5]. Banerjee S, Arnst KE, Wang Y, Kumar G, Deng S, Yang L, et al., Heterocyclic-Fused Pyrimidines as Novel Tubulin Polymerization Inhibitors Targeting the Colchicine Binding Site: Structural Basis and Antitumor Efficacy, J. Med. Chem 61 (4) (2018) 1704–1718. [PubMed: 29406710]

[6]. Perez EA, Microtubule inhibitors: Differentiating tubulin-inhibiting agents based on mechanisms of action, clinical activity, and resistance, Mol. Cancer Ther 8 (8) (2009) 2086–2095. [PubMed: 19671735]

[7]. Jordan MA, Wilson L, Microtubules as a target for anticancer drugs, Nat. Rev. Cancer 4 (4) (2004) 253–265. [PubMed: 15057285]

[8]. Berrieman HK, Lind MJ, Cawkwell L, Do beta-tubulin mutations have a role in resistance to chemotherapy?, Lancet Oncol 5 (3) (2004) 158–164. [PubMed: 15003198]

[9]. Altorki NK, Markowitz GJ, Gao D, Port JL, Saxena A, Stiles B, et al., The lung microenvironment: an important regulator of tumour growth and metastasis, Nat. Rev. Cancer 19 (1) (2019) 9–31. [PubMed: 30532012]

[10]. Otto T, Sicinski P, Cell cycle proteins as promising targets in cancer therapy, Nat. Rev. Cancer 17 (2) (2017) 93–115. [PubMed: 28127048]

[11]. Orth M, Unger K, Schoetz U, Belka C, Lauber K, Taxane-mediated radiosensitization derives from chromosomal missegregation on tripolar mitotic spindles orchestrated by AURKA and TPX2, Oncogene 37 (1) (2018) 52–62. [PubMed: 28869599]

[12]. Choy H, Pyo H, Kim JS, MacRae R, Role of taxanes in the combined modality treatment of patients with locally advanced non-small cell lung cancer, Expert Opin. Pharmacother 2 (6) (2001) 963–974. [PubMed: 11585012]

[13]. Gottesman MM, Fojo T, Bates SE, Multidrug resistance in cancer: role of ATP-dependent transporters, Nat. Rev. Cancer 2 (1) (2002) 48–58. [PubMed: 11902585]

[14]. Seruga B, Ocana A, Tannock IF, Drug resistance in metastatic castration-resistant prostate cancer, Nat Rev. Clin. Oncol 8 (1) (2011) 12–23. [PubMed: 20859283]

[15]. Callaghan R, Luk F, Bebawy M, Inhibition of the multidrug resistance P-glycoprotein: time for a change of strategy?, Drug Metab. Dispos 42 (4) (2014) 623–631. [PubMed: 24492893]

[16]. Yang R, Mondal G, Ness RA, Arnst K, Mundra V, Miller DD, et al., Polymer conjugate of a microtubule destabilizer inhibits lung metastatic melanoma, J Control. Release 249 (2017) 32–41. [PubMed: 28130039]

[17]. Gligorov J, Lotz JP, Preclinical pharmacology of the taxanes: implications of the differences, Oncologist 9 Suppl 2 (2004) 3–8.

[18]. Chen JJ, Ahn S, Wang J, Lu Y, Dalton JT, Miller DD, et al., Discovery of Novel 2-Aryl-4-benzoyl-imidazole (ABI-III) Analogues Targeting Tubulin Polymerization As Antiproliferative Agents, J. Med. Chem 55 (16) (2012) 7285–7289. [PubMed: 22783954]

[19]. Wang QH, Arnst KE, Wang YX, Kumar G, Ma DJ, Chen H, et al., Structural Modification of the 3,4,5-Trimethoxyphenyl Moiety in the Tubulin Inhibitor VERU-111 Leads to Improved Antiproliferative Activities, J. Med. Chem 61 (17) (2018) 7877–7891. [PubMed: 30122035]

[20]. Kashyap VK, Wang Q, Setua S, Nagesh PKB, Chauhan N, Kumari S, et al., Therapeutic efficacy of a novel beta III/beta IV-tubulin inhibitor (VERU-111) in pancreatic cancer, J. Exp. Clin. Cancer Res 38 (1) (2019).

[21]. Deng S, Krutilina RI, Wang Q, Lin Z, Parke DN, Playa HC, et al., An Orally Available Tubulin Inhibitor, VERU-111, Suppresses Triple-Negative Breast Cancer Tumor Growth and Metastasis and Bypasses Taxane Resistance, Mol. Cancer Ther 19 (2) (2020) 348–363. [PubMed: 31645441]

[22]. Bai Z, Gao M, Zhang H, Guan Q, Xu J, Li Y, et al., BZML, a novel colchicine binding site inhibitor, overcomes multidrug resistance in A549/Taxol cells by inhibiting P-gp function and inducing mitotic catastrophe, Cancer Lett 402 (2017) 81–92. [PubMed: 28576750]

[23]. Kavallaris M, Microtubules and resistance to tubulin-binding agents, Nat. Rev. Cancer 10 (3) (2010) 194–204. [PubMed: 20147901]

[24]. Huber RM, Flentje M, Schmidt M, Pollinger B, Gosse H, Willner J, et al., Simultaneous chemoradiotherapy compared with radiotherapy alone after induction chemotherapy in inoperable stage IIIA or IIIB non-small-cell lung cancer: study CTRT99/97 by the Bronchial Carcinoma Therapy Group, J. Clin. Oncol 24 (27) (2006) 4397–4404. [PubMed: 16983107]

[25]. Holleman A, Chung I, Olsen RR, Kwak B, Mizokami A, Saijo N, et al., miR-135a contributes to paclitaxel resistance in tumor cells both in vitro and in vivo, Oncogene 30 (43) (2011) 4386–4398. [PubMed: 21552288]

[26]. Chen J, Wang Z, Li CM, Lu Y, Vaddady PK, Meibohm B, et al., Discovery of novel 2-aryl-4-benzoyl-imidazoles targeting the colchicines binding site in tubulin as potential anticancer agents, J. Med. Chem 53 (20) (2010) 7414–7427. [PubMed: 20919720]

[27]. Chen J, Li CM, Wang J, Ahn S, Wang Z, Lu Y, et al., Synthesis and antiproliferative activity of novel 2-aryl-4-benzoyl-imidazole derivatives targeting tubulin polymerization, Bioorg. Med. Chem 19 (16) (2011) 4782–4795. [PubMed: 21775150]

[28]. Lu Y, Chen J, Xiao M, Li W, Miller DD, An overview of tubulin inhibitors that interact with the colchicine binding site, Pharm. Res 29 (11) (2012) 2943–2971. [PubMed: 22814904]

[29]. Li CM, Lu Y, Chen J, Costello TA, Narayanan R, Dalton MN, et al., Orally bioavailable tubulin antagonists for paclitaxel-refractory cancer, Pharm. Res 29 (11) (2012) 3053–3063. [PubMed: 22760659]

[30]. Martello LA, Verdier-Pinard P, Shen HJ, He L, Torres K, Orr GA, et al., Elevated levels of microtubule destabilizing factors in a Taxol-resistant/dependent A549 cell line with an alpha-tubulin mutation, Cancer Res 63 (6) (2003) 1207–1213. [PubMed: 12649178]

[31]. Gan PP, Pasquier E, Kavallaris M, Class III beta-tubulin mediates sensitivity to chemotherapeutic drugs in non small cell lung cancer, Cancer Res 67 (19) (2007) 9356–9363. [PubMed: 17909044]

[32]. Li L, Jiang S, Li X, Liu Y, Su J, Chen J, Recent advances in trimethoxyphenyl (TMP) based tubulin inhibitors targeting the colchicine binding site, Eur. J. Med. Chem 151 (2018) 482–494. [PubMed: 29649743]

[33]. Dlugosz A, Janecka A, ABC Transporters in the Development of Multidrug Resistance in Cancer Therapy, Curr. Pharm. Des 22 (30) (2016) 4705–4716. [PubMed: 26932159]

[34]. Lo YC, Cormier O, Liu T, Nettles KW, Katzenellenbogen JA, Stearns T, et al., Pocket similarity identifies selective estrogen receptor modulators as microtubule modulators at the taxane site, Nat. Commun 10 (1) (2019) 1033. [PubMed: 30833575]

[35]. Mahmud F, Jeon OC, Alam F, Maharjan R, Choi JU, Park J, et al., Oral pemetrexed facilitates low-dose metronomic therapy and enhances antitumor efficacy in lung cancer, J. Control. Release 284 (2018) 160–170. [PubMed: 29908222]

[36]. Thanki K, Gangwal RP, Sangamwar AT, Jain S, Oral delivery of anticancer drugs: challenges and opportunities, J. Control. Release 170 (1) (2013) 15–40. [PubMed: 23648832]

[37]. Rowinsky EK, Eisenhauer EA, Chaudhry V, Arbuck SG, Donehower RC, Clinical toxicities encountered with paclitaxel (Taxol), Semin. Oncol 20 (4) (1993) 1–15.

[38]. Mahmud F, Chung SW, Alam F, Choi JU, Kim SW, Kim IS, et al., Metronomic chemotherapy using orally active carboplatin/deoxycholate complex to maintain drug concentration within a tolerable range for effective cancer management, J. Control. Release 249 (2017) 42–52. [PubMed: 28093298]

Highlights

- VERU-111 targets the colchicine site in tubulin and circumvents P-glyprotein overexpression mediated drug resistance in NSCLC
- Orally administrated VERU-111 significantly inhibits both parental A549 and highly paclitaxel-resistant A549/TxR tumor growth *in vivo*.
- Combination therapy of VERU-111 and cisplatin improves the anti-tumor efficacy in A549/TxR cells by inducing apoptosis

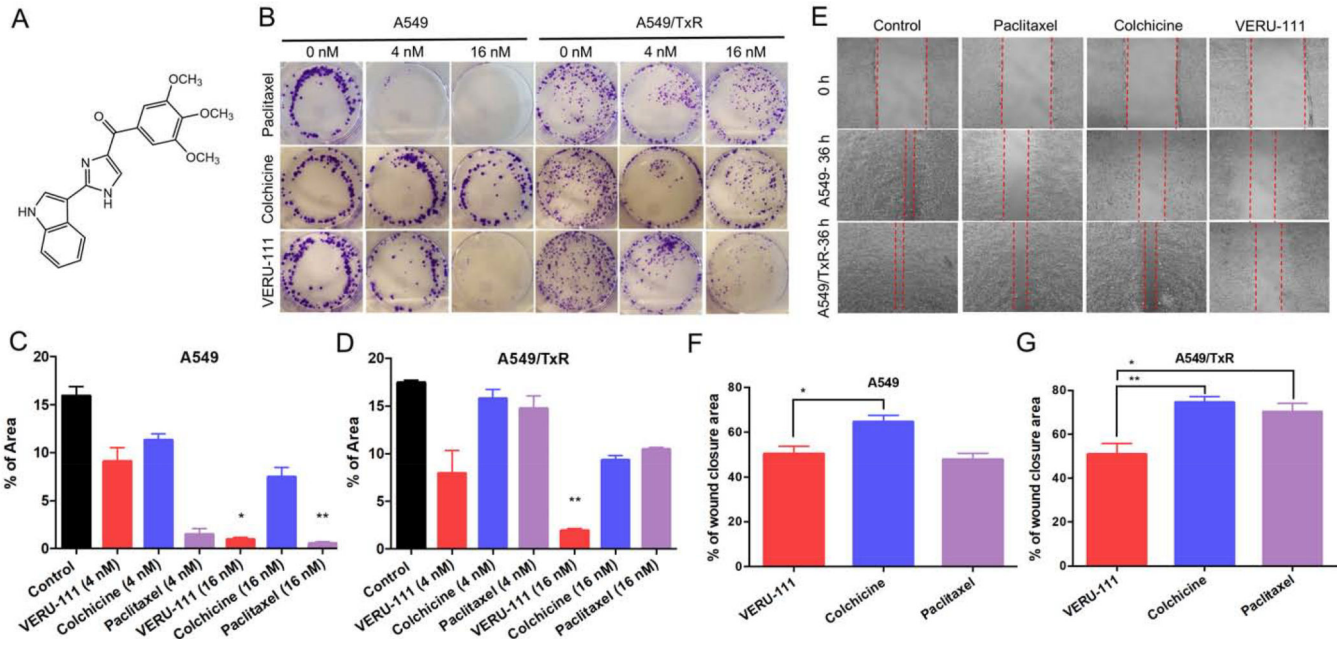

Figure 1:

The cell colony formation and migration effects of VERU-111 on A549 and A549/TxR cells. (A) Chemical structure of VERU-111 ((2-(1H-Indol-3-yl)-1H-imidazol-4-yl)(3,4,5-trimethoxyphenyl) Methanone) (B) Representative images from the colony formation assay, (C-D) The quantification of the results from colony area in A549 and A549/TxR cells. The experiment was conducted using two different drug concentrations (4 nM and 16 nM) in a 6-well plate. ImageJ software was used to calculate the total colony occupied area. (E) Would healing assay was done in 12-well plates and the drug solutions were incubated for 36 hours to observe the effects of VERU-111 in compared with positive controls (colchicine and paclitaxel). (F-G) The total scratched area that covered with migrated cells was quantified and represented as percent of total wound closure area. The data is presented as mean ± SEM of triplicates and the Kruskal-Wallis test was performed for the statistical significance. $*p < 0.05$, $**p < 0.01$ versus control or indicated.

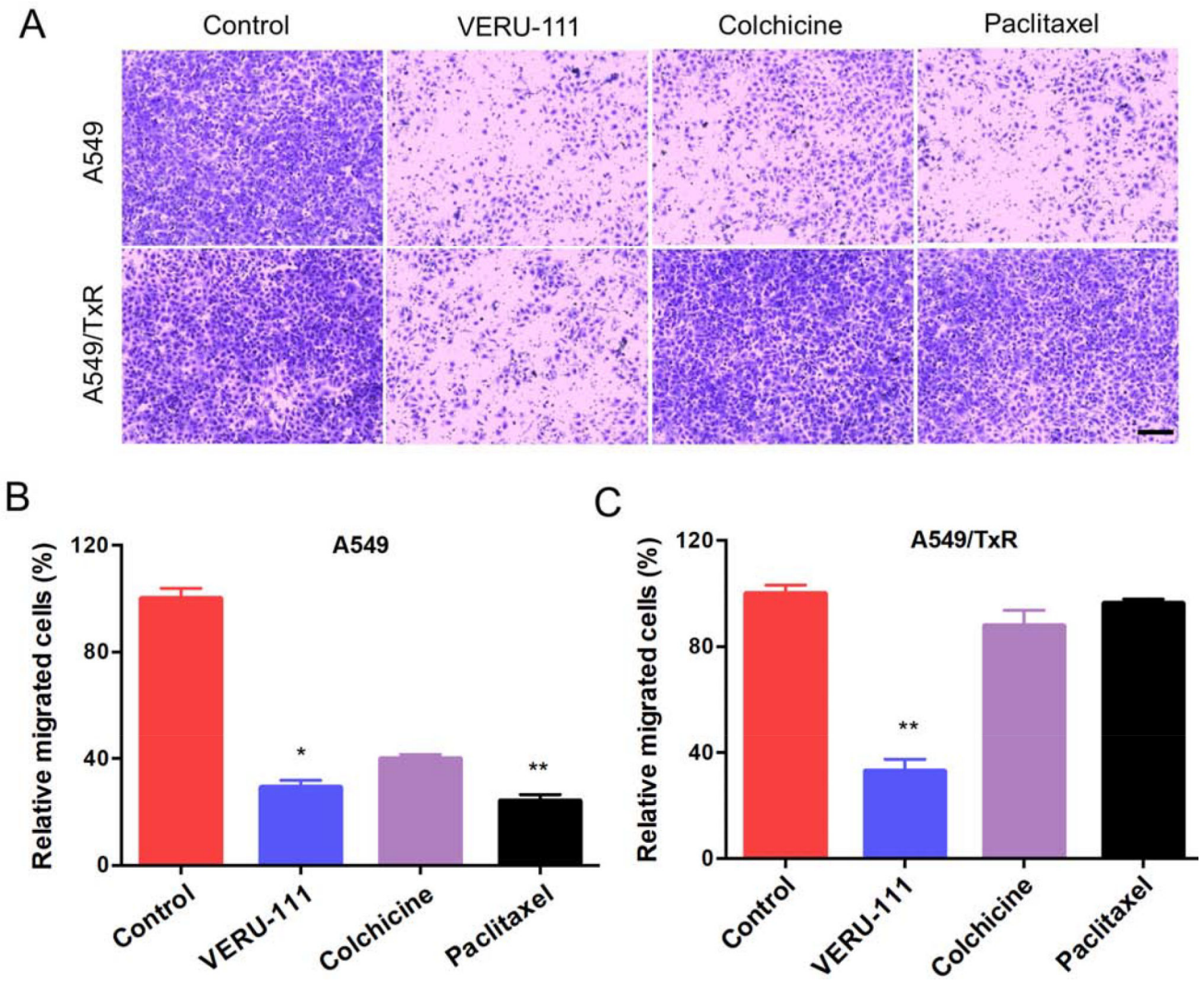

Figure 2:

The effects of VERU-111 on cell invasion in A549 and A549/TxR cells. (A) Images showing the invaded cells after treatment with VERU-111, colchicine and paclitaxel from the matrigel-coated surface to lower chamber, (B-C) The relative number cells compared with control invaded from apical to basolateral side were quantified and plotted. The data is presented as mean ± SEM (n =4) and the Kruskal-Wallis test was performed for the statistical significance. *$p < 0.05$, **$p < 0.01$ versus control or indicated. Scale bar: 200 μm.

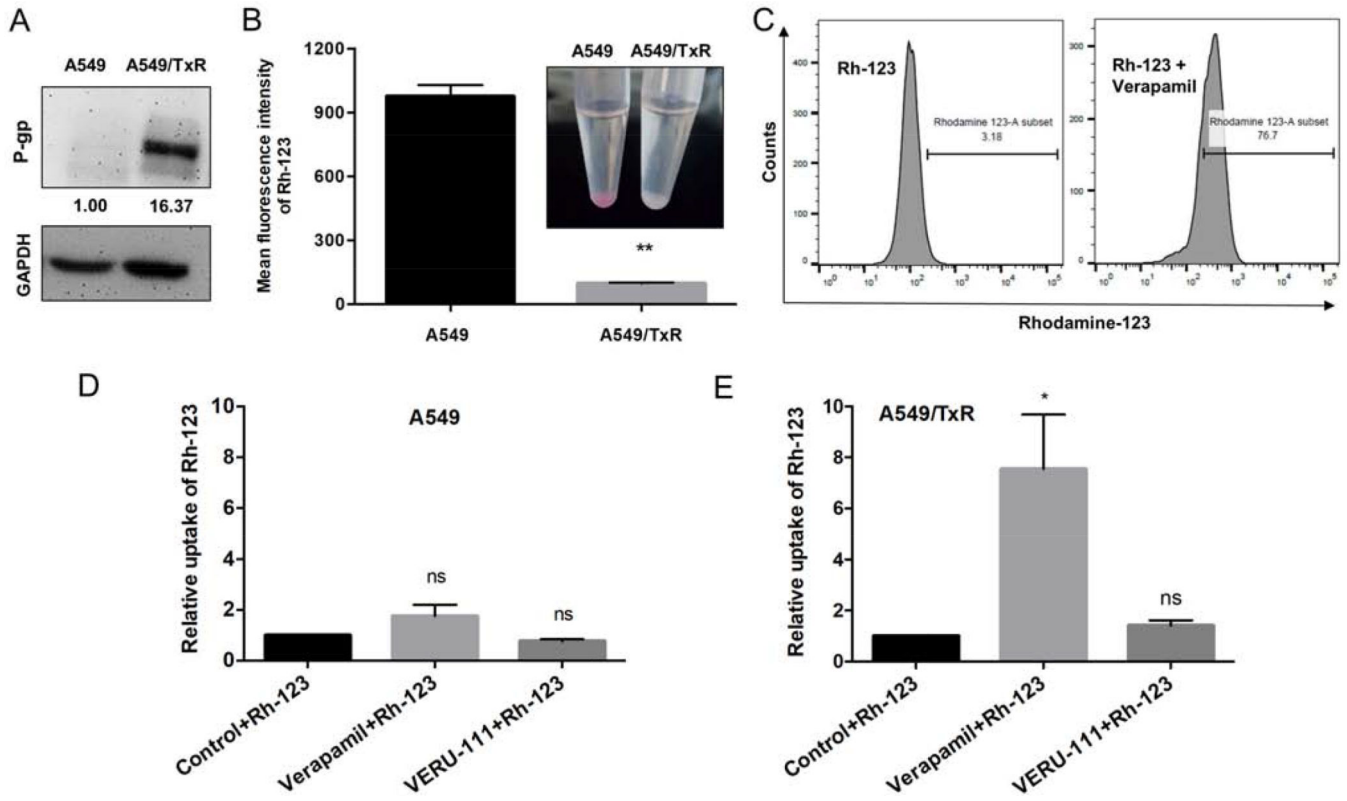

Figure 3:

VERU-111 may bypass P-gp efflux transporter in paclitaxel-resistant cells. (A) Comparison of P-gp expression on sensitive and resistant A549 cells by western blotting. (B) Rhodamine-123, a substrate for P-gp, had lower accumulation in resistant cells by using flow cytometry. (C) Verapamil, another positive substrate for P-gp, blocks the efflux transporter, and thereby increased accumulation of rhodamine-123 into the A549/TxR cells. (D-E) Comparison of rhodamine-123 accumulation in the presence of verapamil or VERU-111 in A549 and A549/TxR cell lines. The data is presented as mean ± SEM of triplicates and the unpaired *t* test with Welch's correction or Dunnett multiple comparisons were performed for the statistical significance. ns = not significant, $*p < 0.05$, $**p < 0.01$ versus control or indicated.

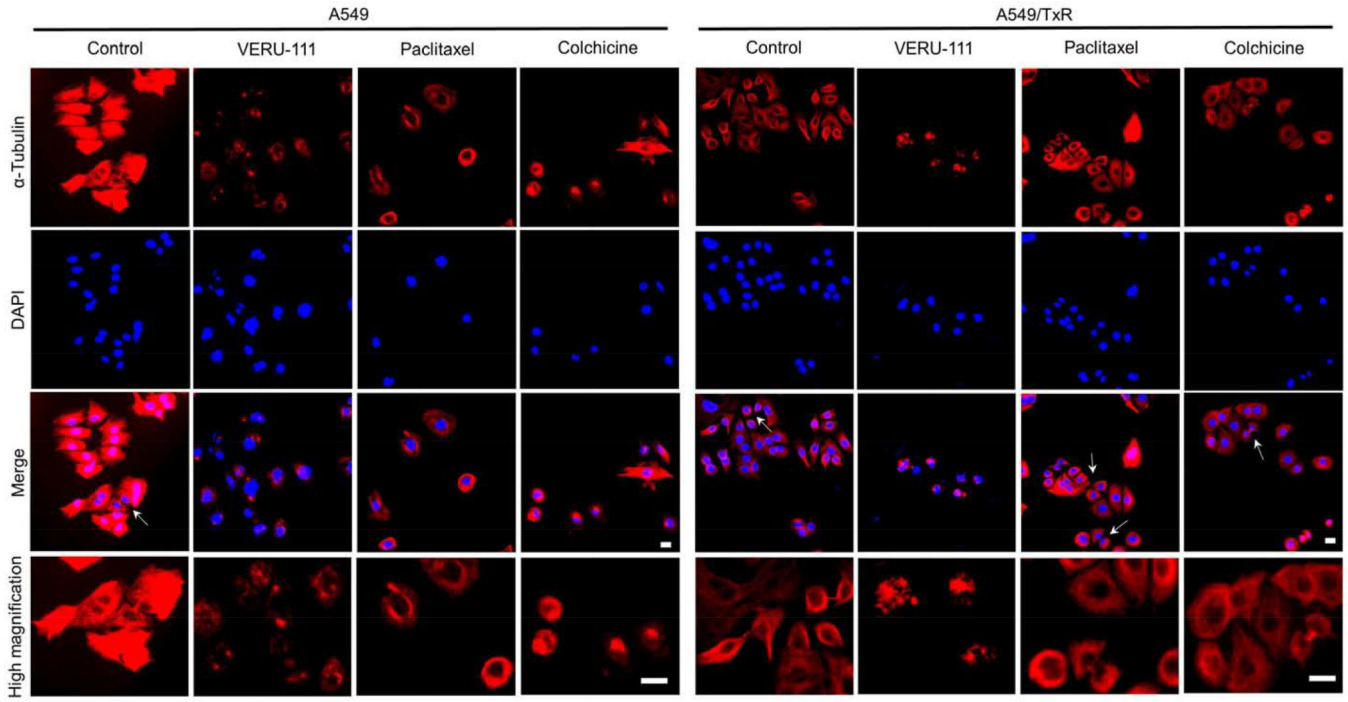

Figure 4:

Immunofluorescence staining showing the microtubules networks were disrupted after treatment with VERU-111, paclitaxel or colchicine compared with control cells. Both A549 and A549/TxR cells were used in this study to evaluate the drug-induced effects (100 nM for 24 h) on microtubules which were visualized with anti-α-tubulin antibody (red) and the nuclei with DAPI staining. The photographs were captured by fluorescence microscopy and the white arrows were pointed for cytokinesis. Scale bar: 20 μm.

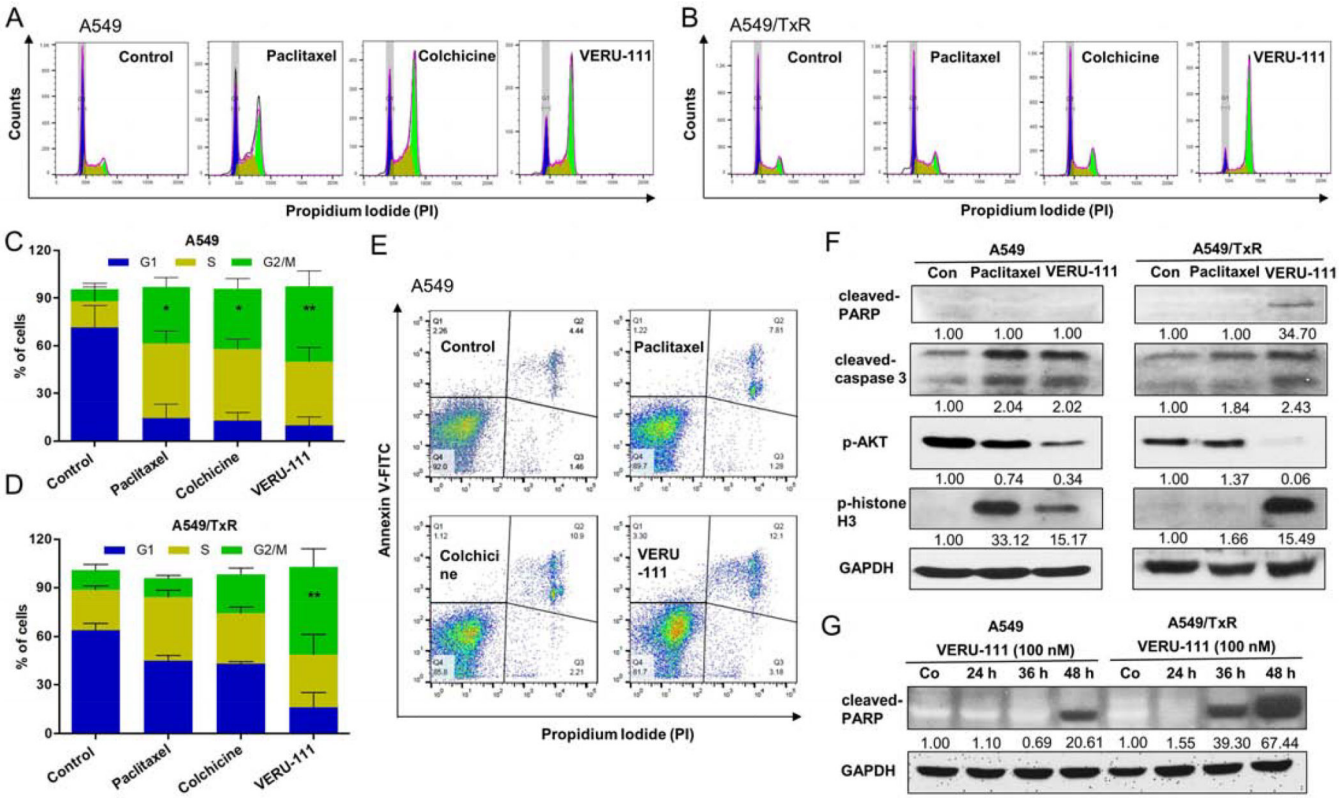

Figure 5:

VERU-111 induces the cell death in A549 and A549/TxR cells. Flow cytometry (FACS) analysis using PI staining showed the cell cycle arrest of G2/M phase by VERU-111 or positive controls in (A) A549 cells or (B) A549/TxR cells after adding 100 nM drug concentration for 24 h. (C-D) The quantitative analysis from figure A and B. The cells were fixed with 70% ethanol and treated with RNase A. (E) VERU-111 displayed highest apoptosis induction in parenteral A549 cells among all groups by annexin V-FITC/PI staining of live single cells. (F) Protein levels of caspase-3 and PARP cleavage, AKT phosphorylation and phosphorylation of histone H3 were identified by western blot assay after treatment with 100 nM paclitaxel or 100 nM VERU-111 for 24 h. GAPDH was used as a loading control. (G) PARP cleavage by western blot following VERU-111 treatment (100 nM) for 24, 36 and 48 h. GAPDH was used as a loading control. Signal intensity was evaluated by Image Studio Lite densitometry, with control group set to 1.00. The data is presented as mean ± SEM of triplicates and Dunnett multiple comparisons were performed for the statistical significance. $*p < 0.05$, $**p < 0.01$ versus control or indicated.

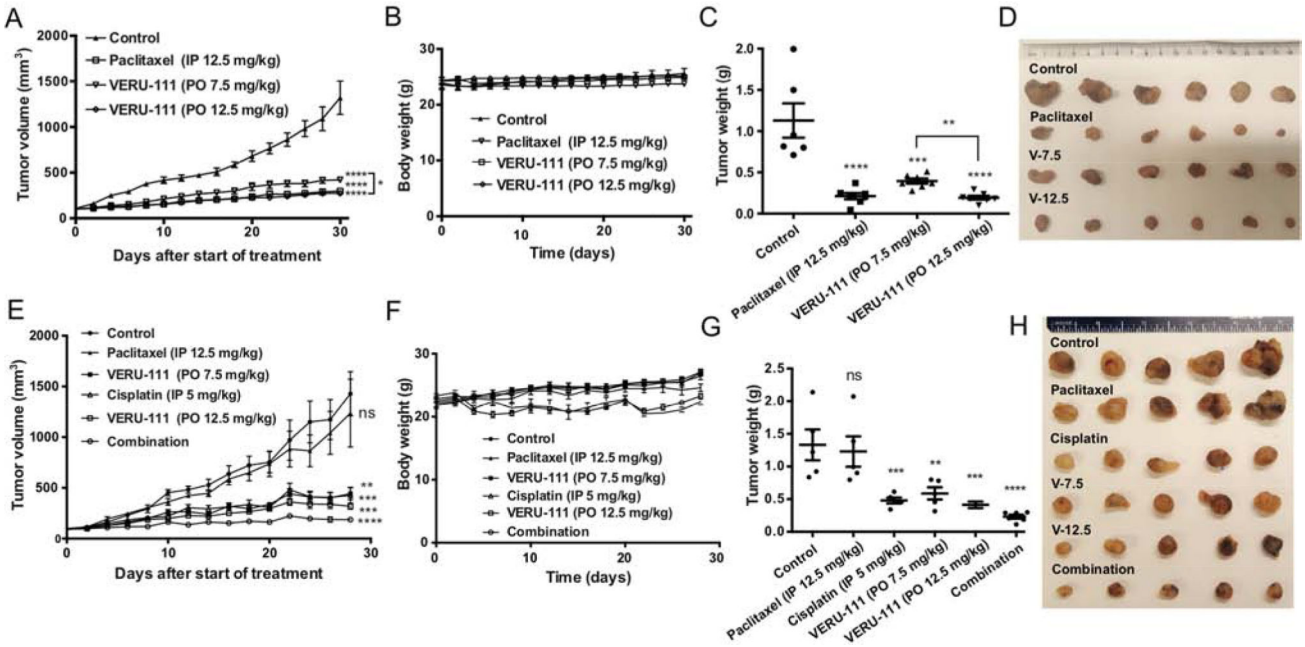

Figure 6:

Antitumor efficacy study of VERU-111 in A549 and A549/TxR animal models. Athymic nude mice received 7.5 mg/kg or 12.5 mg/kg oral dose (po) of VERU-111 every five days in a week and 12.5 mg/kg paclitaxel intraperitoneal (ip) injection for three alternate days in a week. The drug treatment was started when the tumor volume reached to 100 mm3 and indicated at day 0 in these graphs. (A) A549 xenografted mice showed significant inhibition of tumor growth in all treated groups. (B) There was no significant change in body weight. (C) The weight of the tumors also significantly lower than control. (D) The photograph of individual tumors from all groups. (E) Xenograft study showing A549/TxR resistant tumor volume after treatment with various treatment groups. Cisplatin was injected at a dose of 5 mg/kg ip once in a week. The combination group received 12.5 mg/kg po of VERU-111 and 5 mg/kg ip of cisplatin. (F) Only cisplatin therapy alone or in combination with VERU-111 showed slight reduction of mice body weight. (G) The quantitative analysis of the tumor weight from different groups. (H) The tumor photographs showing no response in tumor size in control and paclitaxel group. Data represented as the mean ± SEM (n=5–7). Statistical analysis was performed by Dunnett multiple comparisons test. *$p < 0.05$, **$p < 0.01$, ***$p < 0.001$, ****$p < 0.0001$ versus control or indicated.

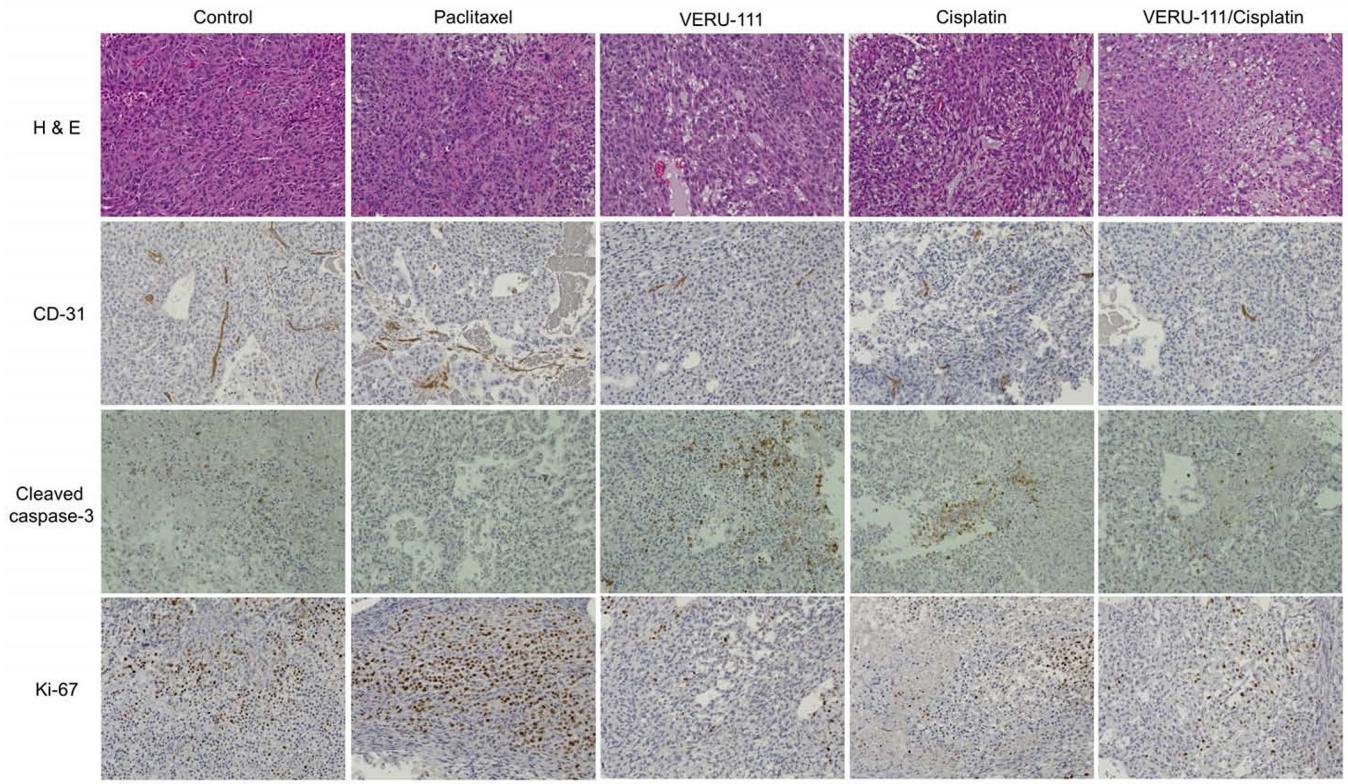

Figure 7:

Effect of VERU-111, paclitaxel, cisplatin or in combination of VERU-111 and cisplatin treatment on A549/TxR tumor growth and apoptosis. Tumor tissues were stained with hematoxylin and eosin (H&E), endothelial cells marker CD-31 antibody, apoptosis marker cleaved-caspase-3 antibody or proliferation marker Ki-67 and the representative images were shown. Images were captured at 20x magnification.

Table 1:

Cytotoxic effects of microtubule targeting agents against various human lung cancer cell lines (mean ± SEM, n = 6–8).

Cell lines	Paclitaxel IC_{50} (nM)	Colchicine IC_{50} (nM)	VERU-111 IC_{50} (nM)
H1299	0.37 ± 0.09	30.26 ± 5.98	35.79 ± 8.49
H460	73.55 ± 11.92	40.52 ± 4.81	178.00 ± 33.48
HCC827	4.23 ± 1.14	17.59 ± 6.31	28.98 ± 11.41
A549	18.80 ± 2.37	109.00 ± 22.72	55.61 ± 11.21
A549/TxR	5411.00 ± 534.59	728.50 ± 176.04	102.90 ± 18.40
RI	287.82	6.68	1.85

Note: IC_{50}; The half maximal inhibitory concentration, RI; the resistance index between A549 and A549/TxR cell lines.